

Revealing the A_{1g}-type strain effect on superconductivity and nematicity in FeSe thin flake

Zhaohui Cheng(程朝晖), Bin Lei(雷彬), Xigang Luo(罗习刚), Jianjun Ying(应剑俊), Zhenyu Wang(王震宇), Tao Wu(吴涛), and Xianhui Chen(陈仙辉)

Citation: Chin. Phys. B, 2021, 30 (**9**): 097403. DOI: 10.1088/1674-1056/ac1efa
Journal homepage: http://cpb.iphy.ac.cn; http://iopscience.iop.org/cpb

What follows is a list of articles you may be interested in

Anomalous spectral weight transfer in the nematic state of iron-selenide superconductor

C Cai(蔡淙), T T Han(韩婷婷), Z G Wang(王政国), L Chen(陈磊), Y D Wang(王宇迪), Z M Xin(信子鸣), M W Ma(马明伟), Yuan Li(李源), Y Zhang(张焱)

Chin. Phys. B, 2020, 29 (**7**): 077401. DOI: 10.1088/1674-1056/ab90ec

Crystal structures and sign reversal Hall resistivities in iron-based superconductors $Li_x(C_3H_{10}N_2)_{0.32}FeSe$ ($0.15 < x < 0.4$)

Rui-Jin Sun(孙瑞锦), Shi-Feng Jin(金士锋), Jun Deng(邓俊), Mu-Nan Hao(郝木难), Lin-Lin Zhao(赵琳琳), Xiao Fan(范晓), Xiao-Ning Sun(孙晓宁), Jian-Gang Guo(郭建刚), Lin Gu(谷林)

Chin. Phys. B, 2019, 28 (**6**): 067401. DOI: 10.1088/1674-1056/28/6/067401

Nonlinear uniaxial pressure dependence of the resistivity in $Sr_{1-x}Ba_xFe_{1.97}Ni_{0.03}As_2$

Hui-Can Mao(毛慧灿), Dong-Liang Gong(龚冬良), Xiao-Yan Ma(马肖燕), Hui-Qian Luo(罗会仟), Yi-Feng Yang(杨义峰), Lei Shan(单磊), Shi-Liang Li(李世亮)

Chin. Phys. B, 2018, 27 (**8**): 087402. DOI: 10.1088/1674-1056/27/8/087402

Comparison of band structure and superconductivity in $FeSe_{0.5}Te_{0.5}$ and FeS

Yang Yang(杨阳), Shi-Quan Feng(冯世全), Yuan-Yuan Xiang(向圆圆), Hong-Yan Lu(路洪艳), Wan-Sheng Wang(王万胜)

Chin. Phys. B, 2017, 26 (**12**): 127401. DOI: 10.1088/1674-1056/26/12/127401

Fluctuating specific heat in two-band superconductors

Lei Qiao(乔雷), Cheng Chi(迟诚), Jiangfan Wang(王江帆)

Chin. Phys. B, 2017, 26 (**11**): 117401. DOI: 10.1088/1674-1056/26/11/117401

RAPID COMMUNICATION

Revealing the A_{1g}-type strain effect on superconductivity and nematicity in FeSe thin flake*

Zhaohui Cheng(程朝晖)[1], Bin Lei(雷彬)[1], Xigang Luo(罗习刚)[1,2], Jianjun Ying(应剑俊)[1,3], Zhenyu Wang(王震宇)[1,3], Tao Wu(吴涛)[1,2,3,5,†], and Xianhui Chen(陈仙辉)[1,2,3,4,5]

[1] *CAS Key Laboratory of Strongly-coupled Quantum Matter Physics, Department of Physics, University of Science and Technology of China, Hefei* 230026, *China*

[2] *Hefei National Laboratory for Physical Sciences at the Microscale, University of Science and Technology of China, Hefei* 230026, *China*

[3] *CAS Center for Excellence in Superconducting Electronics (CENSE), Shanghai* 200050, *China*

[4] *CAS Center for Excellence in Quantum Information and Quantum Physics, Hefei* 230026, *China*

[5] *Collaborative Innovation Center of Advanced Microstructures, Nanjing University, Nanjing* 210093, *China*

(Received 12 August 2021; revised manuscript received 16 August 2021; accepted manuscript online 19 August 2021)

The driving mechanism of nematicity and its twist with superconductivity in iron-based superconductors are still under debate. Recently, a dominant B_{1g}-type strain effect on superconductivity is observed in underdoped iron-pnictides superconductors $Ba(Fe_{1-x}Co_x)_2As_2$, suggesting a strong interplay between nematicity and superconductivity. Since the long-range spin order is absent in FeSe superconductor, whether a similar strain effect could be also observed or not is an interesting question. Here, by utilizing a flexible film as substrate, we successfully achieve a wide-range-strain tuning of FeSe thin flake, in which both the tensile and compressive strain could reach up to $\sim 0.7\%$, and systematically study the strain effect on both superconducting and nematic transition (T_c and T_s) in the FeSe thin flake. Our results reveal a predominant A_{1g}-type strain effect on T_c. Meanwhile, T_s exhibits a monotonic anti-correlation with T_c and the maximum T_c reaches to 12 K when T_s is strongly suppressed under the maximum compressive strain. Finally, in comparison with the results in the underdoped $Ba(Fe_{1-x}Co_x)_2As_2$, the absence of B_{1g}-type strain effect in FeSe further supports the role of stripe-type spin fluctuations on superconductivity. In addition, our work also supports that the orbital degree of freedom plays a key role to drive the nematic transition in FeSe.

Keywords: iron-based superconductors, superconductivity, electronic nematicity, strain effect

PACS: 74.70.Xa, 74.25.F−, 77.80.bn **DOI:** 10.1088/1674-1056/ac1efa

Electronic nematic phase, in which the rotational symmetry is broken, exhibits a twist with superconductivity in the electronic phase diagram of iron-based superconductors (IBSCs).[1] Many experiments have already shown conclusive evidences for the electronic nematicity in IBSCs, including anisotropic transport, angle resolved photoemission spectroscopy (ARPES), scanning tunneling microscopy (STM), neutron scattering and so on.[2] So far, although the existence of electronic nematicity in IBSCs is well-established,[3–5] the underlying mechanism and its exact role on the superconducting pairing are still mystery and under hot debate.[1,6,7] Most of the existing experimental results support a direct competition between nematic order and superconductivity in the electronic phase diagram.[8,9] Since the nematic order is tightly twisted with a stripe-type antiferromagnetic order in the iron-pnictide family,[10–12] the competition between the nematic order and the superconductivity is widely believed to stem from the competition between antiferromagnetic order and superconductivity.[8,9] In this case, the nematic order is even considered to be driven by stripe-type spin fluctuations.[1,5,13–16] However, in iron-selenides family such as $FeSe_{1-x}S_x$ systems, there is no direct evidence for the competition between nematic order and superconductivity.[17,18] Interestingly, the stripe-type antiferromagnetic order is also decoupled with nematic order in the electronic phase diagram, which leads to an alternative scenario for electronic nematicity due to orbital order,[19,20] e.g., the ferro-orbital order. Moreover, orbital fluctuations are also considered to mediate an s^{++} superconducting pairing.[21] So far, the origin of the electronic nematicity and its role on superconductivity are still highly controversial in iron-selenides family.[1,6,7,21,22]

As a conjugate field for electronic nematicity, strain can be used to manipulate the electronic nematicity,[3–5,24,25] which is helpful to elucidate the relationship between electronic nematicity and superconductivity.[26,27] Recently, a dominant B_{1g}-type strain effect on superconductivity has been revealed in the underdoped $Ba(Fe_{1-x}Co_x)_2As_2$.[24,25] With further electron doping, an A_{1g}-type instead of B_{1g}-type

*Project supported by the National Key R&D Program of China (Grant Nos. 2017YFA0303000 and 2016YFA0300201), the National Natural Science Foundation of China (Grant No. 11888101), the Strategic Priority Research Program of Chinese Academy of Sciences (Grant No. XDB25000000), and the Anhui Initiative in Quantum Information Technologies (Grant No. AHY160000).

†Corresponding author. E-mail: wutao@ustc.edu.cn

© 2021 Chinese Physical Society and IOP Publishing Ltd

strain effect appears and becomes dominant in the overdoped $Ba(Fe_{1-x}Co_x)_2As_2$.[28,29] These results strongly support a significant role of electronic nematicity on superconductivity. Then, a natural question is whether a similar B_{1g}-type strain effect could be also observed in iron-selenides family or not, which would be helpful to further understand the role of electronic nematicity on the superconducting pairing in IBSCs.

Previous study on FeSe thin films, utilizing pulsed laser deposition on different substrates, already indicates that the superconducting transition temperature (T_c) in FeSe thin films is highly tunable from 0 K to 12 K by changing the lattice parameters.[30] However, the previous study of the strain effect on T_c in bulk FeSe is not very successful due to the possible damage of FeSe single crystals by large uniaxial strain.[2] Only a small range of uniaxial strain could be applied to FeSe single crystal through a "horseshoe device" or pasting on a piezo-ceramic stack to achieve the measurements of nematic susceptibility.[31,32] In this work, in order to increase the tuning range of uniaxial strain in the bulk FeSe, we adopt a mechanical cleavage method to first cleave FeSe single crystal into thin flakes with the thickness of ~ 25 nm, and then transfer these FeSe thin flakes on a flexible substrate. The uniaxial strain is applied to these thin flakes by bending the flexible substrate. The similar method has been successfully used for the strain tuning of MoS_2 and black phosphorus thin flakes.[33,34] By utilizing this method for applying uniaxial strain, T_c and T_s of FeSe thin flakes can be largely varied exceeding all previous studies on the strain effect in bulk FeSe. The maximum T_c of FeSe can be increased by 30% through applying a compressive strain up to 12 K, while the nematic transition temperature shows an anti-correlation with T_c. Detailed measuring procedures and data analysis are presented in the following part. We note that, during preparing this manuscript, a couple of similar researches on the strain-tuning effects of bulk FeSe have been published.[35–37] The strain-tuning methods in these researches are different from ours, while the main results are consistent with our experiments.

In order to achieve continuous change of the uniaxial strain, we use flexible polyethylene terephthalate (PET) films as the substrate to stick FeSe thin flakes and then bend the substrate to produce strain. Bending the flexible substrate downward/upward could induce a tensile/compressive strain on the FeSe thin flakes (Fig. 1(b)). The nominal magnitude of the strain is defined as $\varepsilon = \Delta L/L_0$, where $\Delta L = L - L_0$, and L_0 and L are the sample length without and with strain, respectively (see supplementary materials for the details of calculation).

As shown in Fig. 1(a), due to the van der Waals interaction between different FeSe layers, the FeSe thin flakes can be easily obtained by the mechanical exfoliation with scotch tape method. FeSe thin flakes are first mechanically exfoliated from bulk crystals onto polydimethylsiloxane (PDMS) substrates, and then transferred to PET substrates by the so-called

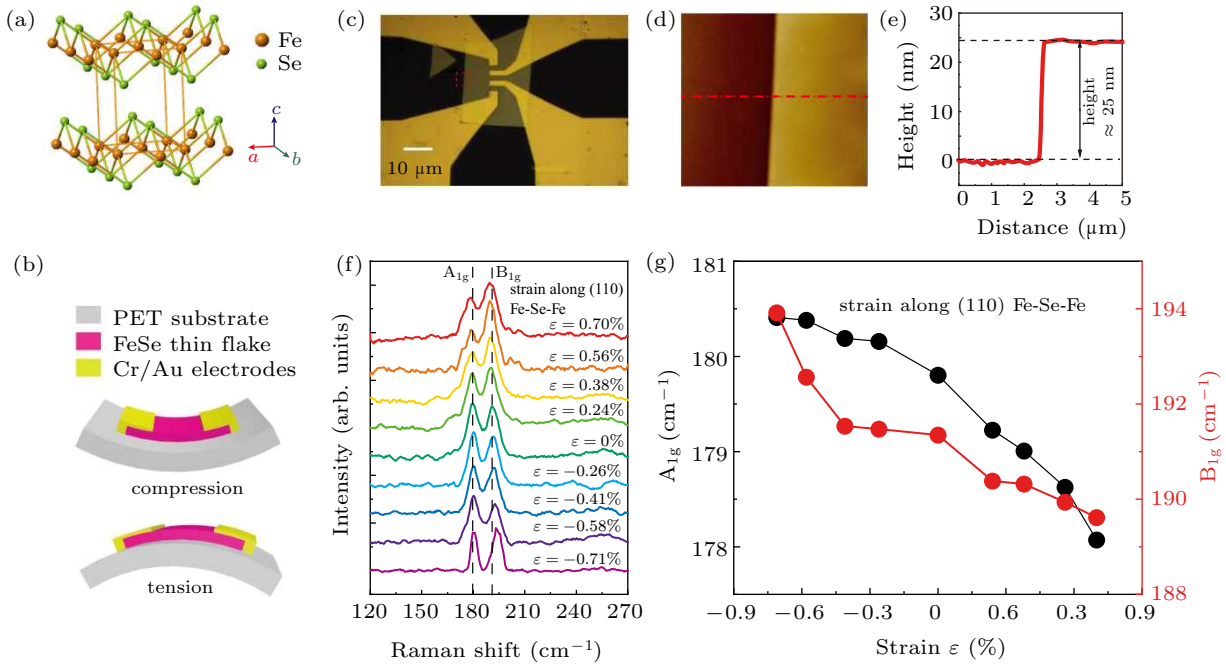


Fig. 1. Crystal structure, device configuration and strain-dependent Raman spectra of FeSe. (a) The crystal structure of the pristine FeSe. (b) Schematic structure of a FeSe thin flake on the flexible polyethylene terephthalate (PET) substrate. Variable compressive/tensile strains are induced on FeSe thin flakes by bending the substrate downward/upward. (c) An optical image of a FeSe thin flake supported on flexible PET substrate. (d), (e) AFM image of the dashed square in (c). The thickness of FeSe thin flake is about 25 nm along the red dashed line. (f) *In-situ* Raman spectroscopy of the FeSe thin flakes under different tensile and compressive strains with the strain along (110). The peaks of A_{1g} and B_{1g} modes move to the lower wave number with increasing the tensile strain and shift to the higher wave number with increasing the compressive strain. (g) The peak positions of A_{1g} and B_{1g} modes as a function of the strain. The frequencies of the A_{1g} and B_{1g} modes monotonously decrease with increasing the strain from negative to positive.

dry-transfer method.[38] (see supplementary materials for the details of devices fabrication). Figure 1(b) is the schematic structure of the final strain device. In practical, proper thin flakes with good flatness and regular shape are chosen by using an optical microscopy. Then, the thickness is characterized by an atomic force microscopy (AFM). The typical thickness of the FeSe thin flakes used for the transport measurement is about 25 nm as evidenced by the AFM image as shown in Figs. 1(d) and 1(e). Finally, four electrodes (Cr/Au with thicknesses of 5 and 50 nm, respectively) for transport measurements are coated on the surface of the FeSe thin flakes by using mask technique. The coated four electrodes also serve as the clamping points to prevent the sample from slippage during the bending of the substrate. Figure 1(c) displays an optical image of the actual device. It should be noted that the in-plane crystal orientation of FeSe single crystal is determined by Laue diffraction measurement. The applied strain by bending the PET substrate is always along the [110] or [100] direction. The direction of the current can be changed by varying the direction of the electrodes.

The strain induced by bending the PET substrate can be estimated by a continuum-mechanics model for an elastic beam (see supplementary material S2), in which the radius of curvature (R) from the bending of the PET substrate is assumed to be much larger than the thickness (h) of the PET substrate. Then, the magnitude of the applied strain can be calculated by $\varepsilon = h/2R$ [39] (see details in Fig. S1 of the supplementary materials). A positive/negative ε denotes a tensile/compressive strain, respectively. In this work, the thickness of the PET substrate is about 100 μm, and we could extract the value of R from the profile of the bended PET substrate. In order to continuously change the strain in the FeSe thin flakes, the prepared device is fixed in the middle of two parallel plates and the distance between these two plates is continuously changed to bend the PET substrate. If no slippage happens between the FeSe thin flake and PET substrate, then the strain ε in the FeSe thin flake can be directly calculated by the above formula. Here, the sample should be mounted in the middle position of the substrate.

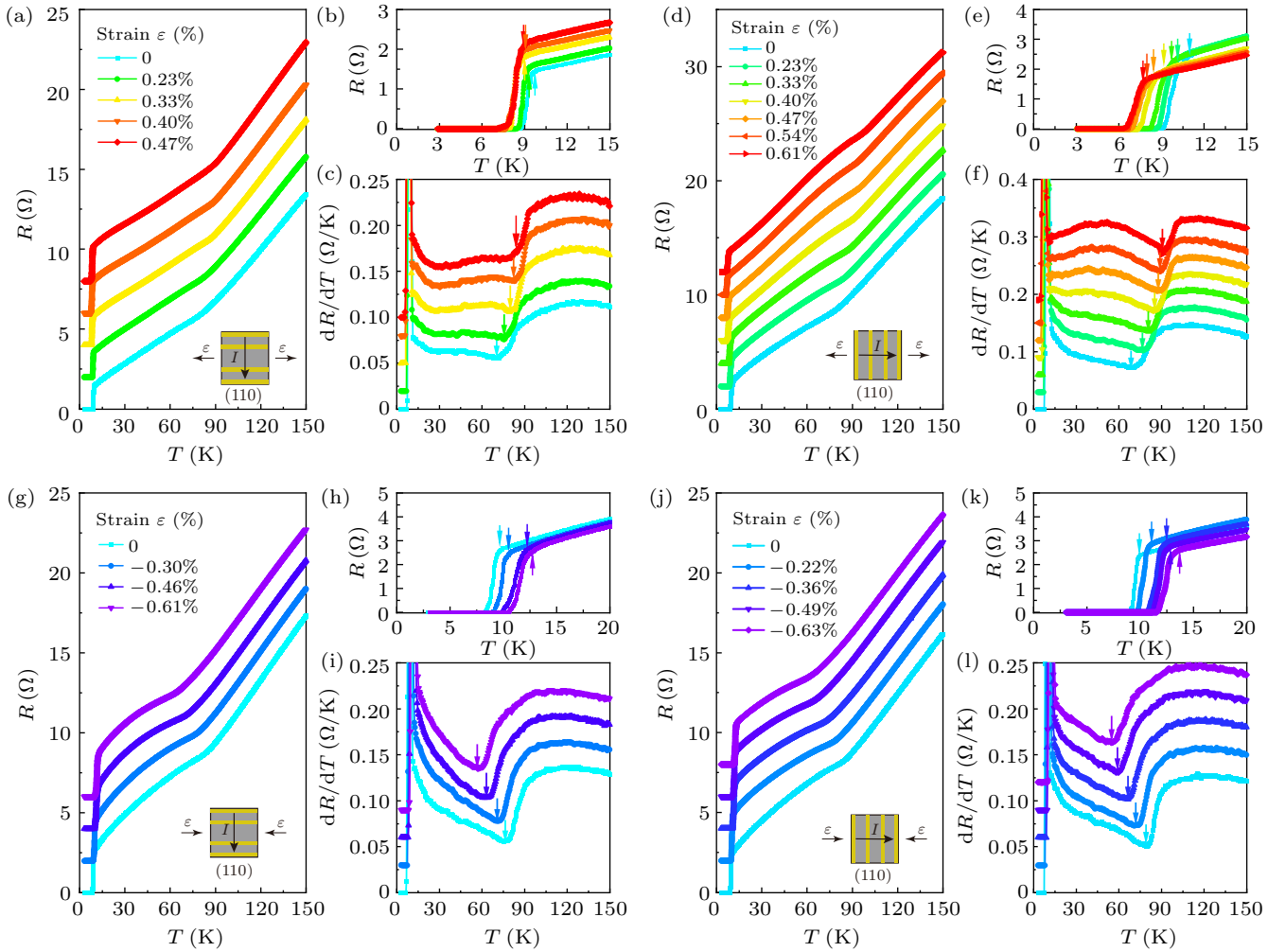


Fig. 2. The longitudinal resistance and the temperature derivatives of the resistance at different ε along (110). (a), (d), (g) and (j) Temperature dependence of resistance for FeSe thin flakes under different strains and different current directions. The inset is a schematic of the strain and the direction of the measured current. (b), (e), (h) and (k) The resistance at low temperatures corresponding to (a), (d), (g) and (j). (c), (f), (i) and (l) Temperature dependence of the temperature derivative of resistance for the samples corresponding to (a), (d), (g) and (j).

Usually, x-ray diffraction (XRD) experiment is needed to verify the change of lattice parameters due to uniaxial strain. However, due to limited sample's volume, it is very difficult to perform an *in-situ* XRD measurement on the FeSe thin flakes as that in large single crystal.[40] Instead, we have performed *in-situ* Raman measurements, which is sensitive to uniaxial strains on the FeSe thin-flake samples. As shown in Fig. 1(f), we successfully obtain *in-situ* Raman spectra for the FeSe thin flakes under various strains along [110] direction. The A_{1g} and B_{1g} modes come from the vibrations of Se atoms along the *c* axis and the vibrations of Fe atoms along the *c* axis, respectively.[41–43] By increasing the strain from tensile to compressive strain, both A_{1g} and B_{1g} modes continuously shift to a higher wavenumber. The systematic evolution of A_{1g} and B_{1g} modes with the uniaxial strain is shown in Fig. 1(g). Qualitatively, although the absolute magnitude of the uniaxial strain on the FeSe thin flakes can not be determined precisely, the *in-situ* Raman result indicates that the uniaxial strain by bending the PET substrate is effectively transferred to the FeSe thin flakes. Similar *in-situ* Raman results are also obtained in the FeSe thin flakes under various strains along [100] direction (see supplementary materials Fig. S3). Therefore, we assume that the calculated value of strain by the above mentioned method well represents the actual strain in the FeSe thin flakes. Next, we would investigate the strain effects on both superconducting and nematic transitions in the FeSe thin flakes by electronic transport measurements.

As shown in Fig. 2, the temperature dependence of resistance for the FeSe thin flakes are systematically measured under different strains along the [110] (Fe–Se–Fe) direction. In order to measure both tensile/compressive strain effects with the electric current parallel or perpendicular to the bending direction, we have prepared four similar strain devices to measure the temperature-dependent resistance. Figures 2(a) and 2(d) show the temperature dependences of resistances under tensile strain, with the electric current parallel and perpendicular to the direction of the uniaxial strain, respectively. The overall temperature dependence of resistance is very similar to the previous report on the bulk FeSe,[18] excepting a higher superconducting temperature and a lower nematic transition temperature. Such difference in superconducting and nematic temperatures between bulk FeSe and FeSe thin flake has already been reported in previous study.[44] Moreover, with increasing the tensile strain, the temperature-dependent resistances show a clear difference below the nematic transition temperature with current parallel and perpendicular to [110] direction, which suggests that the FeSe thin flake on the PET substrate is detwinned with the applied tensile substrate. The superconducting temperature (defined as the middle point of the resistive transition T_c^{mid}) drops from the initial 9 K to 7.8 K with a tensile strain up to 0.47% in the device, when the electric current flows perpendicular to the direction of uniaxial strain. In the device with the electric current parallel to the direction of uniaxial strain, T_c^{mid} drops from the initial 9.6 K to 6.9 K with a tensile strain up to 0.61%. In spite of slightly difference between different devices, it is clear that the superconducting temperature is almost linearly suppressed by increasing the tensile strain along the [110] direction. On the other hand, the nematic transition temperature (T_s) is determined from the derivative of the temperature-dependent resistance. As shown in Figs. 2(c) and 2(f), there is a clear sharp jump due to the nematic transition in the differential curves. T_s is determined by the minimum of the jump. In the device with current parallel to the direction of uniaxial strain, T_s gradually increases from initial 71.2 K to 91.2 K with a tensile strain up to 0.61%. In the device with current perpendicular to the direction of uniaxial strain, T_s gradually increases from initial 70.4 K to 83 K with a tensile strain up to 0.47%. Therefore, in contrast to the superconducting temperature, the nematic transition temperature is clearly increased as the tensile strain increases.

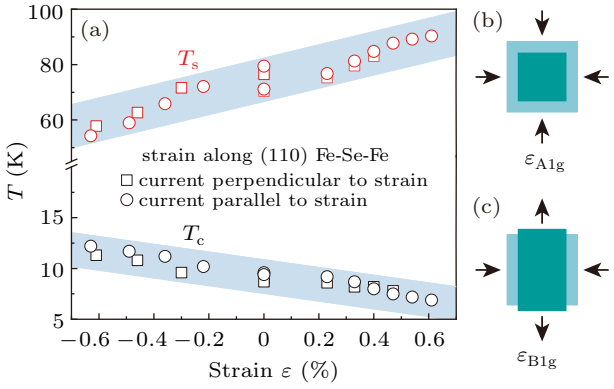


Fig. 3. (a) T_c and T_s as a function of the strain ε when the strain is applied along the [110] direction. With increasing the tensile strain, T_c gradually decreases and T_s gradually increases. With increasing the compressive strain, T_c gradually increases and T_s gradually decreases. There is a negative correlation between T_c and T_s. (b) and (c) Schematics of different strain types. $\varepsilon_{A_{1g}}$ is symmetry-preserving strain and $\varepsilon_{B_{1g}}$ is the strain component which breaks the four-fold rotational symmetry.

As shown in Figs. 2(g) and 2(j), the compressive strain effect on both superconducting and nematic transition temperatures has also been measured with electric current parallel or perpendicular to the direction of uniaxial strain. In the device with electric current parallel to the direction of uniaxial strain, T_c^{mid} increases from the initial 9.4 K to 12.2 K and T_s decreases from the initial 79.5 K to 54.3 K with the compressive strain up to −0.63%. In the device with electric current perpendicular to the direction of uniaxial strain, T_c^{mid} increases from the initial 8.7 K to 11.3 K and T_s decreases from the initial 76.5 K to 57.8 K with the compressive strain up to −0.61%. Totally, the compressive strain effect is similar to the above observed tensile strain effect, and we could summarize all these results

and plot the overall strain dependence of T_s and T_c with different uniaxial strains. As shown in Fig. 3, under uniaxial strains along the [110] direction, T_c increases while T_s decreases and the correlation between T_c and T_s follows a universal linear behavior with current parallel or perpendicular to the strain. Interestingly, a similar result is also observed under uniaxial strain along the [100] direction (more details see the supplementary materials Figs. S4 and S5). Then, a natural question is how to understand the strain effect on both T_c and T_s.

In general, a uniaxial stress applied along one in-plane direction (a or b axis) will induce strains along all three principal axes.[28] Then we have $\varepsilon_{jj} = -v_{ij}\varepsilon_{ii}$, where v_{ij} is the intrinsic Poisson ratio for materials. This gives

$$\varepsilon_{\mathrm{B1g}} = 1/2(\varepsilon_{aa} - \varepsilon_{bb}) = 1/2\varepsilon_{aa}(1 + v_{ab}), \quad (1)$$

$$\varepsilon_{\mathrm{A1g_1}} = 1/2(\varepsilon_{aa} + \varepsilon_{bb}) = 1/2\varepsilon_{aa}(1 - v_{ab}), \quad (2)$$

$$\varepsilon_{\mathrm{A1g_2}} = \varepsilon_{cc} = -\varepsilon_{aa}v_{ac}, \quad (3)$$

where $\varepsilon_{\mathrm{A1g_1}}$ and $\varepsilon_{\mathrm{A1g_2}}$ are the non-symmetry-breaking strain such as volume expansion and change of tetragonality; and $\varepsilon_{\mathrm{B1g}}$ is the strain component which breaks the four-fold rotational symmetry. Based on symmetry considerations, T_c should depend quadratically on $\varepsilon_{\mathrm{B2g}}$ but linearly on $\varepsilon_{\mathrm{A1g}}$. Accordingly, we have[28]

$$T_c(\varepsilon) = T_c(0)\left(1 + \beta\varepsilon_{\mathrm{A1g}} - \frac{1}{2}\alpha\varepsilon_{\mathrm{B1g}}^2\right), \quad (4)$$

where α and β are the dimensionless coefficients of the dependence of T_c on $\varepsilon_{\mathrm{A1g}}$ and $\varepsilon_{\mathrm{B1g}}$, respectively. In the previous study on the underdoped $Ba(Fe_{1-x}Co_x)_2As_2$, the strain-dependent T_c is found to be dominant by a $\varepsilon_{\mathrm{B1g}}$ component and shows a quadratical dependence. In that case, the coefficient of the quadratic term α is believed to be related to the long-range antiferromagnetic order existing in $Ba(Fe_{1-x}Co_x)_2As_2$ and $\varepsilon_{\mathrm{B1g}}$ would enhance spin fluctuations while suppress nematic fluctuations.[45] With increasing the amount of Co doping to the overdoped region, the antiferromagnetic order in $Ba(Fe_{1-x}Co_x)_2As_2$ is gradually suppressed and then $\varepsilon_{\mathrm{A1g}}$ becomes dominant on the strain dependence of T_c. Following this explanation on strain-dependent T_c, the absence of long-range antiferromagnetic order in bulk FeSe would lead to a negligible value of α and then only a linear term would be left. This is definitely confirmed by the observation in the present study. Therefore, our results indirectly support a role of stripe-type spin fluctuations on superconductivity. In addition, as reported in previous literatures, T_c is found to be very sensitive to the change of the c-axis lattice constant in FeSe thin films,[27] which might be responsible for the observed predominant A_{1g}-type strain effect. In fact, the A_{1g}-type strain effect could be also compared with the pressure effect in FeSe, in which the superconducting transition temperature would be enhanced by low pressure below 1 GPa while the nematic transition temperature is suppressed. However, with further increasing pressure, a long-range antiferromagnetic order would appear and then T_c would be slightly suppressed by the development of antiferromagnetic order.[46] Here, whether a long-range antiferromagnetic order would appear or not with further increasing strain is still elusive. It may deserve further study to clarify the underlying physics for the A_{1g}-type strain effect. On the other hand, a similar B_{1g}-type strain effect on the nematic transition temperature was also revealed in the underdoped $Ba(Fe_{1-x}Co_x)_2As_2$.[28] However, our results clearly demonstrate that such a B_{1g}-type strain effect on T_s is absent in FeSe. If assuming a key role of spin degree of freedom on the electronic nematicity in iron-pnictides, the absence of B_{1g}-type strain effect on T_s suggests that the orbital degree of freedom might play a key role instead of the spin degree of freedom to drive the electronic nematicity. Since the orbital order is sensitive to the change of lattice parameter,[47–49] the dominant A_{1g}-type strain effect on T_s could be also related to the change of lattice parameter induce by uniaxial strain as that for T_c. Therefore, combining the strain effect in both FeSe and $Ba(Fe_{1-x}Co_x)_2As$, the stripe-type spin fluctuations, which would lead to a B_{1g}-type strain effect on both T_c and T_s, play a more important role than orbital fluctuations on the superconductivity in IBSCs. In fact, this is also supported by a slight change of T_c across the nematic quantum critical point in $FeSe_{1-x}S_x$ system.[25] Recently, several experiments on the strain-tuning effects of bulk FeSe have been conducted by different groups.[35–37] Owing to different measuring methods and sample dimensions, there is a few slight differences in the detailed behavior of $T_s(\varepsilon)$ and $T_c(\varepsilon)$ among different experiments.[35–37] Nevertheless, consistent conclusions are obtained, which suggest intrinsic strain-tuning effects revealed in this study.

In summary, by utilizing PET substrate, we successfully obtain a wide-range strain tuning for FeSe thin flake with both tensile and compressive strain up to about 0.7%. Our results reveal a predominant A_{1g}-type strain effect on T_c, which is different from that of B_{1g}-type in underdoped $Ba(Fe_{1-x}Co_x)_2As_2$. Meanwhile, T_s exhibits a monotonic anti-correlation with T_c and the maximum T_c reaches to 12 K when T_s is strongly suppressed under the maximum compressive strain. Finally, in comparison with the results in the underdoped $Ba(Fe_{1-x}Co_x)_2As_2$, the absence of B_{1g}-type strain effect in FeSe further supports a role of stripe-type spin fluctuations on superconductivity. Our findings provide new insights for clarifying the underlying mechanism of nematic order and its twist with superconductivity in iron-based superconductors.

References

[1] Fernandes R M and Schmalian J 2012 *Supercond. Sci. Technol.* **25** 084005
[2] Bohmer A E and Kreisel A 2018 *J. Phys.: Condens. Matter* **30** 023001
[3] Chu J H, Analytis J G, Greve K D, McMahon P L, Islam Z, Yamamoto Y and Fisher I R 2010 *Science* **329** 824
[4] Tanatar M A, Blomberg E C, Kreyssig A, Kim M G, Ni N, Thaler A, Budko S L, Canfield P C, Goldman A I, Mazin I I and Prozorov R 2010 *Phys. Rev. B* **81** 184508
[5] Fisher I R, Degiorgi L and Shen Z X 2011 *Rep. Prog. Phys.* **74** 124506
[6] Fernandes R M, Chubukov A V and Schmalian J 2014 *Nat. Phys.* **10** 97
[7] Chubukov A V, Khodas M, and Fernandes R M 2016 *Phys. Rev. X* **6** 041045
[8] Kim H, Tanatar M A, Straszheim W E, Cho K, Murphy J, Spyrison N, Reid J P, Shen B, Wen H H, Fernandes R M and Prozorov R 2014 *Phys. Rev. B* **90** 014517
[9] Nandi S, Kim M G, Kreyssig A, Fernandes R M, Pratt D K, Thaler A, Ni N, Bud'ko S L, Canfield P C, Schmalian J, McQueeney R J and Goldman A I 2010 *Phys. Rev. Lett.* **104** 057006
[10] Fang C, Yao H, Tsai W F, Hu J and Kivelson S A 2008 *Phys. Rev. B* **77** 224509
[11] Xu C, Müller M and Sachdev S 2008 *Phys. Rev. B* **78** 020501(R)
[12] Fernandes R M, VanBebber L H, Bhattacharaya S, Chandra P, Keppens P, Mandrus D, McGuire M A, Sales B C, Sefat A S and Schmalian J 2010 *Phys. Rev. Lett.* **105** 157003
[13] Song Y, Lu X Y, Abernathy D L, Tam D W, Niedziela J L, Tian W, Luo H Q, Si Q M and Dai P C 2015 *Phys. Rev. B* **92** 180504
[14] Yi M, Lu D H, Chu J H, Analytis J G, Sorini A P, Kemper A F, Moritz B, Moore R G, Hashimoto M, Lee W S, Hussain Z, Devereaux T P, Fisher I R and Shen Z X 2011 *Proc. Natl. Acad. Sci. USA* **108** 6878
[15] Lu X Y, Park J T, Zhang R, Luo H Q, Nevidomskyy A H, Si Q M and Dai P C 2014 *Science* **345** 657
[16] Zhang W L, Park J T, Lu X Y, Wei Y, Ma X Y, Hao L J, Dai P C, Meng Z Y, Yang Y F, Luo H Q and Li S L 2016 *Phys. Rev. Lett.* **117** 227003
[17] Nabeshima F, Ishikawa T, Oyanagi K I, Kawai M and Maeda A 2018 *J. Phys. Soc. Jpn.* **87** 073704
[18] Licciardello S, Buhot J, Lu J, Ayres J, Kasahara S, Matsuda Y, Shibauchi T and Hussey N E 2019 *Nature* **567** 213
[19] Baek S H, Efremov D V, Ok J M, Kim J S, Brink J and Büchner B 2015 *Nat. Mater.* **14** 210
[20] Fanfarillo L, Mansart J, Toulemonde P, Cercellier H, Le Fèvre P, Bertran F, Valenzuela B, Benfatto L and Brouet V 2016 *Phys. Rev. B* **94** 155138
[21] Saito T, Onari S and Kontani H 2011 *Phys. Rev. B* **83** 140512
[22] Kreisel A, Hirschfeld P J and Andersen B M 2020 *Symmetry* **12** 1402
[23] Benfatto L, Valenzuela B and Fanfarillo L 2018 *Npj Quantum Mater.* **3** 56
[24] Chu J H, Kuo H H, Analytis J G and Fisher I R 2012 *Science* **337** 710
[25] Hosoi S, Matsuura K, Ishida K, Wang H, Mizukami Y, Watashige T, Kasahara S, Matsuda Y and Shibauchi T 2016 *Proc. Natl. Acad. Sci. USA* **113** 8139
[26] Nabeshima F, Imai Y, Hanawa M, Tsukada I and Maeda A 2013 *Appl. Phys. Lett.* **103** 172602
[27] Feng Z P, Yuan J, He G, Hu W, Lin Z F, Li D, Jiang X Y, Huang Y L, Ni S L, Li J, Zhu B Y, Dong X L, Zhou F, Wang H B, Zhao Z X and Jin K 2018 *Sci. Rep.* **8** 4039
[28] Malinowski P, Jiang Q N, Sanchez J J, Mutch J, Liu Z Y, Went P, Liu J, Ryan P J, Kin J W, and Chu J H 2020 *Nat. Phys.* **16** 1189
[29] Worasaran T, Ikeda M S, Palmstrom J C, Straquadine J A W, Kivelson S A and Fisher I R 2021 *Science* **372** 973
[30] Feng Z P, Yuan J, Li J, Wu X X, Hu W, Shen B, Qin M Y, Zhao L, Zhu B Y, Stanev V, Liu M, Zhang G M, Yang H X, Li J Q, Dong X L, Zhou F, Zhou X J, Kusmartsev F V, Hu J P, Takeuchi I, Zhao Z X and Jin K 2019 arXiv:1807.01273
[31] Tanatar M A, Böhmer A E, Timmons E I, Schütt M, Drachuck G, Taufour V, Kothapalli K, Kreyssig A, Bud'ko S L, Canfield P C, Fernandes R M and Prozorov R 2016 *Phys. Rev. Lett.* **117** 127001
[32] Hosoi S, Matsuura K, Ishida K, Wang H, Mizukami Y, Watashige T, Kasahara S, Matsuda Y and Shibauchi T 2016 *Proc. Natl. Acad. Sci. USA* **113** 8139
[33] Conley H J, Wang B, Ziegler J I, Haglund R F, Pantelides J S and Bolotin K I 2013 *Nano Lett.* **13** 3626
[34] Zhang Z C, Li L K, Horng J, Wang N Z, Yang F Y, Yu Y J, Zhang Y, Chen G R, Watanabe K, Taniguchi T, Chen X H, Wang F and Zhang Y B 2017 *Nano Lett.* **17** 6097
[35] Bartlett J M, Steppke A, Hosoi S, Noad H, Park J, Timm C, Shibauchi T, Mackenzie A P and Hicks C W 2021 *Phys. Rev. X* **11** 021038
[36] Ghini M, Bristow M, Prentice J C A, Sutherland S, Sanna S, Haghighirad A A and Coldea A I 2021 *Phys. Rev. B* **103** 205139
[37] Nakajima M, Ohata Y and Tajima S 2021 *Phys. Rev. Mat.* **5** 044801
[38] Kinoshita K, Moriya R, Onodera M, Wakafuji Y, Masubuchi S, Watanabe K, Taniguchi T and Machida T 2019 *Npj 2D Mater. Appl.* **3** 22
[39] Roldán R, Castellanos-Gomez A, Cappelluti E and Guinea F 2015 *J. Phys. Condens. Matter* **27** 313201
[40] Lei B, Wang N Z, Shang C, Meng F B, Ma L K, Luo X G, Wu T, Sun Z, Jiang Z, Mao B H, Liu Z, Yu Y J, Zhang Y B and Chen X H 2017 *Phys. Rev. B.* **95** 020503
[41] Xia T L, Hou D, Zhao S C, Zhang A M, Chen G F, Luo J L, Wang N L, Wei J H, Lu Z Y and Zhang Q M 2009 *Phys. Rev. B* **79** 140510
[42] Gnezdilov V, Pashkevich Y G, Lemmens P, Wulferding D, Shevtsova T, Gusev A, Chareev D and Vasiliev A 2013 *Phys. Rev. B* **87** 144508
[43] Zhang A M, Ma X L, Wang Y M, Sun S S, Lei B, Lei H C, Chen X H, Wang X Q, Chen C F and Zhang Q M 2019 *Phys. Rev. B* **100** 060504(R)
[44] Zhang Y, Yi M, Liu Z K, Li W, Lee J J, Moore R G, Hashimoto M, Nakajima M, Eisaki H, Mo S K, Hussain Z, Devereaux T P, Shen Z X and Lu D H 2016 *Phys. Rev. B* **94** 115153
[45] Kissikov T, Sarkar R, Lawson M, Bush B T, Timmons E I, Tanatar M A, Prozorov R, Bud'ko S L, Canfield P C, Fernandes R M and Curro N J 2018 *Nat. Commun.* **9** 1058
[46] Sun J P, Matsuura K, Ye G Z, Mizukami Y, Shimozawa M, Matsubayashi K, Yamashita M, Watashige T, Kasahara S, Matsuda Y, Yan J Q, Sales B C, Uwatoko Y, Cheng J G and Shibauchi T 2016 *Nat. Commun.* **7** 12146
[47] Fernandes R M and Chubukov A V 2017 *Rep. Prog. Phys.* **80** 014503
[48] Bendele M, Amato A, Conder K, Elender M, Keller H, Klauss H H, Luetkens H, Pomjakushina E, Raselli A and Khasanov R 2010 *Phys. Rev. Lett.* **104** 087003
[49] Phan G N, Nakayama K, Sugawara K, Sato T, Urata T, Tanabe Y, Tanigaki K, Nabeshima F, Imai Y, Maeda A and Takahashi T 2017 *Phys. Rev. B* **95** 224507